

Can Precision Measurements of Slepton Masses Probe Right Handed Neutrinos?

Howard Baer¹, Csaba Balázs², J. Kenichi Mizukoshi² and Xerxes Tata²

¹*Department of Physics, Florida State University, Tallahassee, FL 32306 USA*

²*Department of Physics and Astronomy, University of Hawaii, Honolulu, HI 96822, USA*

(October 24, 2018)

Abstract

In a supersymmetric model, the presence of a right handed neutrino with a large Yukawa coupling f_ν would affect slepton masses via its contribution to the renormalization group evolution between the grand unification and weak scales. Assuming a hierarchical pattern of neutrino masses, these effects are large for only the third generation of sleptons. We construct mass combinations to isolate the effect of f_ν from mass corrections already expected from tau Yukawa couplings. We then analyze the size of these effects, assuming that the Super-Kamiokande data constrain $0.033 \text{ eV} \lesssim m_{\nu_\tau} \lesssim 0.1 \text{ eV}$ and that neutrino masses arise via a see-saw mechanism. We also explore whether these effects might be detectable in experiments at future e^+e^- linear colliders. We find that $m_{\tilde{\nu}_\tau}$ needs to be measured with a precision of about 2-3% to measure the effect of f_ν if the neutrino and top Yukawa couplings unify at the grand unification scale. In a simple case study, we find a precision of only 6-10% might be attainable after several years of operation. If the neutrino Yukawa coupling is larger, or in more complicated models of neutrino masses, a determination of $\tilde{\tau}_1$ and $\tilde{\nu}_\tau$ masses might provide a signal of a Yukawa interaction of neutrinos.

PACS numbers: 14.80.Ly, 13.85.Qk, 11.30.Pb

I. INTRODUCTION AND MOTIVATION

Supersymmetry [1] is a leading candidate for physics beyond the Standard Model (SM). The Minimal Supersymmetric Standard Model (MSSM) posits a spin zero partner for each SM matter field, and spin half partners for the gauge and Higgs fields. While all the dimensionless couplings of the MSSM are completely determined in terms of known SM couplings, the intractably large number of dimensionful soft SUSY breaking parameters is usually reduced by supplementing the MSSM by simple boundary conditions for their renormalization group (RG) evolution [2]. These boundary conditions are chosen so that flavour changing neutral currents (which are generically large in a theory with many scalars) are suppressed to acceptable levels. The boundary conditions are determined by assumptions about the new physics (concerning mediation of SUSY breaking) at a scale between $\sim 10^3$ TeV and M_{Planck} . Various models (mSUGRA, low energy gauge-mediated SUSY breaking, anomaly-mediated SUSY breaking, gaugino-mediated SUSY breaking), each leading to a characteristic pattern of MSSM soft breaking parameters, have been proposed and analyzed.

Within the MSSM framework, neutrinos are massless and have no Yukawa couplings. Evidence from the Super-Kamiokande experiment [3] strongly suggests that there are neutrino oscillations and, almost certainly, a neutrino mass. The favoured interpretation of these data is $\nu_\mu - \nu_\tau$ oscillations, with $\Delta m^2 \sim 3 \times 10^{-3}$ eV² and near-maximal mixing. The see-saw mechanism [4] provides an elegant way of giving small masses to neutrinos: for each massive neutrino, one needs to introduce a SM gauge singlet chiral superfield \hat{N}^c , whose fermion component is the left handed anti-neutrino. A mass term in the superpotential leads to a Majorana mass M_N for the singlet neutrino as well as a lepton-number violating mass for its scalar partner. This mass may be very large and is expected to be $\sim M_{GUT}$, or even M_{Planck} if the right handed neutrino (RHN) is a singlet of the unifying gauge group. The neutrino also acquires a Dirac mass m_D , proportional to the neutrino Yukawa coupling f_ν , from electroweak symmetry breaking. The physical neutrino mass, which is obtained by diagonalizing the neutrino mass matrix, is then $\simeq m_D^2/M_N$, and can be very small since m_D is comparable to or smaller than the electroweak scale.

Without further assumptions, the neutrino Yukawa coupling is arbitrary. However, in models where top and neutrino Yukawa couplings unify at some high scale¹ we expect $f_\nu \simeq f_t$, so that the physical neutrino mass is $\simeq m_t^2/M_N$. Renormalization effects [5] modify this by a factor $O(1)$, but do not change the order of magnitude of the predicted neutrino mass. These effects are accounted for in our analysis.

The introduction of the RHN [6] and its associated Yukawa coupling would change the predictions for $\tilde{\ell}_L$ and $\tilde{\nu}_L$ masses via new contributions to their RG evolution, but would not (at one loop) affect $\tilde{\ell}_R$ or other sparticle masses. Moreover, if we assume that neutrino masses are hierarchical (as they must be in the GUT model with the simplest see-saw

¹Yukawa unification would occur in $SO(10)$ models since all the matter fields including the RHN belong to a single representation. In the minimal $SO(10)$ model where all the fermions get their mass from one Higgs multiplet, all Yukawa couplings are unified. In more complicated models where the masses of up and down type fermions arise from different Higgs fields, we have unification of top and neutrino Yukawa couplings, and separately unification of bottom and tau Yukawa couplings.

mechanism), the Δm^2 measured by the Super-Kamiokande collaboration is essentially $m_{\nu_\tau}^2$, with the masses of other neutrinos being negligible in comparison. In the rest of this analysis we will therefore assume that, like quark and lepton Yukawa couplings, the neutrino Yukawa coupling of just the third generation is relevant. Since this new coupling can affect just $\tilde{\tau}_L$ and $\tilde{\nu}_\tau$ masses, precision measurements of these masses in future experiments at e^+e^- linear colliders (relative to $\tilde{\tau}_R$ and first generation slepton masses) should yield information about f_ν . An examination of how large these effects might be, and an evaluation of the whether they might be detectable in the future, forms the subject of this study.²

The conceptually simple picture is spoiled by two important effects that are already present in the MSSM. First, the usual tau Yukawa interactions already split stau masses from those of other sleptons, and the effects of these depend on the unknown parameter $\tan\beta$ whose value is difficult to pin down except under special circumstances (*e.g.* when the masses of several Higgs bosons can be measured [8]). Second, the same Yukawa interactions also cause $\tilde{\tau}_L - \tilde{\tau}_R$ mixing, so that $m_{\tilde{\tau}_L}$ and $m_{\tilde{\tau}_R}$ are not the physical masses of the staus.

In the next section, we identify slepton mass combinations that are sensitive to ν_τ Yukawa couplings but not to the usual tau Yukawa interactions, and compare expectations for these within a reference model (mSUGRA) and the same model extended by a RHN. In Section III, we perform a case study to estimate the precision with which these variables might be measured at linear colliders in order to assess whether such measurements might be feasible. We conclude in Sec. IV with a summary of our results and some general remarks about how our conclusions depend on the underlying model for neutrino masses.

II. ISOLATING THE EFFECTS OF THE NEUTRINO YUKAWA COUPLING

Although we will limit ourselves to analyzing the effects of adding a RHN to the mSUGRA framework, the ideas are applicable to any model with a well-defined prediction for slepton masses such as gauge-mediated or anomaly-mediated SUSY breaking models. Of course, the extent to which the ideas can actually be implemented in experiments depends on how well these masses can be measured, and is thus sensitive to details of the model.

The superpotential for the MSSM with a singlet neutrino superfield \hat{N}^c (for just a single generation), is given by

$$\hat{f} = \hat{f}_{MSSM} + f_\nu \epsilon_{ij} \hat{L}^i \hat{H}_u^j \hat{N}^c + \frac{1}{2} M_N \hat{N}^c \hat{N}^c \quad (1)$$

where \hat{N}^c is the superfield whose fermionic component is the left handed anti-neutrino and scalar component is $\tilde{\nu}_R^\dagger$. The soft SUSY breaking terms now include

²While this paper was under preparation, we became aware that the same idea had already been suggested in Ref. [7]. This study did not include intra-generational mixing which spoils the simple picture (see below), and also neglected Yukawa couplings in the charged lepton as well as down type quark sector (the latter are eliminated from our considerations). Finally, our examination goes beyond Ref. [7] in that we also examine whether these effects might actually be measurable in future experiments.

$$\mathcal{L} = \mathcal{L}_{MSSM} - m_{\tilde{\nu}_R}^2 |\tilde{\nu}_R|^2 + \left[A_\nu f_\nu \epsilon_{ij} \tilde{L}^i \tilde{H}_u^j \tilde{\nu}_R^\dagger + \frac{1}{2} B_\nu M_N \tilde{\nu}_R^2 + h.c. \right]. \quad (2)$$

The parameters A_ν , B_ν and $m_{\tilde{\nu}_R}$ are assumed to be comparable to the weak scale, even though the right handed neutrino and its superpartner have a mass close to M_N which is much larger.

The complete set of 1-loop RG equations (RGEs) for the MSSM extended by a RHN may be found in Ref. [9], while the 2-loop ones are presented in Ref. [10]. In Ref. [9], sample sparticle mass spectra are shown with and without the effect of a neutrino Yukawa coupling. The 1-loop RGEs for slepton and left handed sneutrino masses contain contributions from gauge interactions and from Yukawa interactions. The former is generation independent while the latter is significant for just the third generation. Furthermore, this Yukawa contribution contains an additional term from the neutrino Yukawa coupling if the model contains a RHN. We begin by defining the quantities

$$\begin{aligned} \Delta_R &= m_{\tilde{e}_R}^2 - m_{\tilde{\tau}_R}^2, \\ \Delta_L &= m_{\tilde{e}_L}^2 - m_{\tilde{\tau}_L}^2, \end{aligned}$$

where the m_i denote the soft-SUSY breaking mass parameters. Aside from D -terms, these are essentially the sparticle masses for the first two generations. This is not the case for the third generation because of effects of Yukawa interactions. Including effects from the RHN, the 1-loop³ RGEs for these quantities are given by [9],

$$\frac{d\Delta_R}{dt} = \frac{2}{16\pi^2} (2f_\tau^2 X_\tau), \quad (3)$$

$$\frac{d\Delta_L}{dt} = \frac{2}{16\pi^2} (f_\tau^2 X_\tau + f_\nu^2 X_\nu), \quad (4)$$

where $t = \ln Q$, $X_\tau = m_{\tilde{\tau}_L}^2 + m_{\tilde{\tau}_R}^2 + m_{H_d}^2 + A_\tau^2$ and $X_\nu = m_{\tilde{\tau}_L}^2 + m_{\tilde{\nu}_R}^2 + m_{H_u}^2 + A_\nu^2$. Of course, below the scale M_N the theory reduces to the MSSM, and the last term in Eq. (4) is absent. This then implies that in a theory with a RHN,

$$\frac{d}{dt} (2\Delta_L - \Delta_R) = \frac{4}{16\pi^2} f_\nu^2 X_\nu, \quad (5)$$

for $M_{GUT} \geq Q \geq M_N$.

Eq. (5) is the starting point for our analysis. Within mSUGRA, $2\Delta_L - \Delta_R \simeq 0$ since the masses are degenerate at the GUT scale and this quantity does not evolve at 1-loop. In contrast, for a model with a large RHN Yukawa coupling, this quantity could evolve significantly between M_{GUT} and M_N . The value of $2\Delta_L - \Delta_R$ at the weak scale is, of course, its value at $Q = M_N$, since it does not evolve for $Q \leq M_N$.

This is illustrated in Fig. 1, where we show

$$\delta_{LR} \equiv \frac{2\Delta_L - \Delta_R}{(m_{\tilde{e}_L}^2 + m_{\tilde{e}_R}^2 + m_{\tilde{\tau}_L}^2 + m_{\tilde{\tau}_R}^2)/4}, \quad (6)$$

³We present the 1-loop RGEs to explain our strategy. In our numerical analysis, however, 2-loop RGEs are used.

which is just the dimensionless rendition of $2\Delta_L - \Delta_R$ obtained by dividing by the mean squared mass of the relevant four quantities, in (a) the mSUGRA model, and (b) the model with a RHN. In frame (a) we show δ_{LR} for 2400 randomly generated mSUGRA models for the parameter ranges,

$$10 \text{ GeV} \leq m_0 \leq 1500 \text{ GeV}, \quad 10 \text{ GeV} \leq m_{1/2} \leq 500 \text{ GeV}, \quad -1.8m_0 \leq A_0 \leq 1.8m_0, \quad \mu = +, -,$$

while in frame (b) we generate models that contain an additional RHN. For definiteness, we assume that the additional soft SUSY breaking parameters are unified at the GUT scale, and further, that $f_\nu(M_{GUT}) = f_t(M_{GUT})$. Then, the only free parameter is the superpotential mass M_N for the singlet neutrino, which we vary⁴ between 10^5 GeV and $M_{GUT} = 2 \times 10^{16}$ GeV. For every set of model parameters, and for both models, we compute δ_{LR} and plot it against M_N in Fig. 1. Of course, there is no RHN in mSUGRA; in the plot in frame (a), each parameter set is randomly assigned a value of M_N , resulting in the M_N independent distribution of points in this case. The important thing to note is that δ_{LR} is negative and typically smaller in magnitude than 0.01 in frame (a), and essentially always smaller than 0.02. In contrast, in models with a RHN, $\delta_{LR} \sim 0.1-0.6$, except when M_N is very close to M_{GUT} in which case there is no range for RG evolution to occur. This is in keeping with expectations from a single step integration of Eq. (5) which gives,

$$(2\Delta_L - \Delta_R)_{M_N} \approx \frac{4}{16\pi^2} f_\nu^2 X_\nu \ln \frac{M_{GUT}}{M_N},$$

assuming all SUSY breaking parameters with dimensions of mass are comparable.

A. Effects of Stau Mixing

While the idea described above is conceptually simple, the problem as we have already noted is that SM Yukawa interactions cause intra-generational mixing and preclude direct determination of $m_{\tilde{\tau}_L}$ and $m_{\tilde{\tau}_R}$, and hence of δ_{LR} . Motivated by the fact that the lighter (heavier) tau slepton is mainly $\tilde{\tau}_R$ ($\tilde{\tau}_L$) we construct new variables,

$$\begin{aligned} \Delta_1 &= m_{\tilde{e}_R}^2 - m_{\tilde{\tau}_1}^2, \\ \Delta_2 &= m_{\tilde{e}_L}^2 - m_{\tilde{\tau}_2}^2, \\ \Delta_\nu &= m_{\tilde{\nu}_e}^2 - m_{\tilde{\nu}_\tau}^2, \end{aligned}$$

that can, in principle, be directly measured in experiments at future linear colliders. Since $\tilde{\nu}_L - \tilde{\nu}_R$ mixing is negligible, Δ_ν defined above is equal to Δ_L , and we have only introduced it for notational reasons. Unlike the case of soft masses where $SU(2)$ symmetry implied $m_{\tilde{\tau}_L} = m_{\tilde{\nu}_\tau}$, we now have three logically independent ‘‘flavour differences’’ that can be formed (see Eq. (8) below). Notice that the hypercharge D -term contribution to the masses

⁴If we assume a simple see-saw mechanism for neutrino masses, M_N is constrained by Super-Kamiokande data. We will return to this issue later.

always cancels as it is generation-independent. We can now form dimensionless differences δ_{12} , $\delta_{1\nu}$, and $\delta_{12\nu}$ analogous to δ_{LR} defined above:

$$\begin{aligned}\delta_{12} &= \frac{2\Delta_2 - \Delta_1}{(m_{\tilde{e}_L}^2 + m_{\tilde{\nu}_2}^2 + m_{\tilde{e}_R}^2 + m_{\tilde{\tau}_1}^2)/4}, \\ \delta_{1\nu} &= \frac{2\Delta_\nu - \Delta_1}{(m_{\tilde{\nu}_e}^2 + m_{\tilde{\nu}_\tau}^2 + m_{\tilde{e}_R}^2 + m_{\tilde{\tau}_1}^2)/4}, \\ \delta_{12\nu} &= \frac{\Delta_2 + \Delta_\nu - \Delta_1}{(m_{\tilde{e}_L}^2 + m_{\tilde{\nu}_2}^2 + m_{\tilde{\nu}_e}^2 + m_{\tilde{\nu}_\tau}^2 + m_{\tilde{e}_R}^2 + m_{\tilde{\tau}_1}^2)/6},\end{aligned}\tag{7}$$

which, we emphasize, might be directly measurable. In the limit that stau mixing is negligible, the analysis should essentially reduce to that which was previously considered. The issue then is to examine how much stau mixing changes the variables δ_{12} , $\delta_{1\nu}$ and $\delta_{12\nu}$ from their values (close to zero in mSUGRA) in the absence of mixing.

Toward this end, we show each of these quantities in Fig. 2 for the mSUGRA model in the first column, and for the mSUGRA model extended by a RHN in the second column. The plot is made in the same way as Fig. 1. The following features are worthy of note.

- The spread of the points in the mSUGRA model is considerably larger than in Fig. 1. Furthermore, as can most easily be seen from the out-liers, it is largest for δ_{12} and smallest for $\delta_{1\nu}$, and is always negative.
- In contrast to the corresponding situation in Fig. 1, we see that mixing allows some of the δ s (especially δ_{12}) to become negative, and the very clean separation between the two models that we had in the previous figure no longer obtains. From the point of view of distinguishing the framework with a RHN from the mSUGRA framework, it is clear that $\delta_{1\nu}$ is the most effective variable.

To understand why this is the case, we first write,

$$\begin{aligned}2\Delta_2 - \Delta_1 &= 2\Delta_L - \Delta_R + 2(m_{\tilde{\tau}_L}^2 - m_{\tilde{\tau}_2}^2) - (m_{\tilde{\tau}_R}^2 - m_{\tilde{\tau}_1}^2), \\ 2\Delta_\nu - \Delta_1 &= 2\Delta_L - \Delta_R - (m_{\tilde{\tau}_R}^2 - m_{\tilde{\tau}_1}^2), \\ \Delta_2 + \Delta_\nu - \Delta_1 &= 2\Delta_L - \Delta_R + (m_{\tilde{\tau}_L}^2 - m_{\tilde{\tau}_2}^2) - (m_{\tilde{\tau}_R}^2 - m_{\tilde{\tau}_1}^2),\end{aligned}\tag{8}$$

and then note that $m_{\tilde{\tau}_L}^2 - m_{\tilde{\tau}_2}^2 = m_{\tilde{\tau}_1}^2 - m_{\tilde{\tau}_R}^2$ (since the sum of mass squared eigenvalues must be the trace of the stau mass squared matrix), and further, that each of these terms is negative because mixing always decreases (increases) the lowest (highest) eigenvalue. We thus expect that $\tilde{\tau}_L - \tilde{\tau}_R$ mixing effects reduce δ_{12} , $\delta_{1\nu}$ and $\delta_{12\nu}$ in Fig. 2 relative to δ_{LR} in Fig. 1, and further, that this reduction is in the ratio 3:1:2. Since these quantities are all negative within the mSUGRA framework, $\delta_{1\nu}$ in the second row of Fig. 2 provides the cleanest separation. This then requires precise measurements of $m_{\tilde{e}_R}$, $m_{\tilde{\nu}_e}$, $m_{\tilde{\tau}_1}$ and $m_{\tilde{\nu}_\tau}$, the prospects for which we will discuss in the next section. It is worth mentioning that stau mixing effects discussed above are absent in the quantity $3\Delta_\nu - \Delta_1 - \Delta_2$ but its determination requires knowledge of $m_{\tilde{e}_L}$ and $m_{\tilde{\tau}_2}$ as well.

Up to now, we have ignored the Super-Kamiokande measurement $10^{-3} \text{ eV}^2 \leq \Delta m^2 \leq 10^{-2} \text{ eV}^2$ which, assuming an inter-generational hierarchy of neutrino masses, implies

$$0.033 \text{ eV} \leq m_{\nu_\tau} \leq 0.1 \text{ eV}. \quad (9)$$

Within the simplest see-saw model the neutrino mass is given by $m_{\bar{\nu}} = (f_{\nu} v_u)^2 / M_N$, where v_u is the vacuum expectation value of the field h_u responsible for the masses of up-type fermions in the MSSM. This in turn implies that f_{ν} and M_N are strongly correlated. In fact, if $f_{\nu}(M_{GUT}) = f_t(M_{GUT})$ then $m_{\nu} \sim m_t^2 / M_N$, so that values of $M_N \lesssim 10^{14}$ GeV are excluded by the Super-Kamiokande data. Then, from Fig. 2, we see that $\delta_{1\nu}$ has to be determined to within 0.05-0.1 in order to distinguish the RHN model from mSUGRA.

We can, however, repeat the previous analysis ignoring the GUT constraint on Yukawa couplings and treating f_{ν} and M_N as parameters of the RHN model, but instead constrain these to yield m_{ν} in the range (9). As before, we generate random parameter sets for both these models, and then compute δ_{12} , $\delta_{1\nu}$ and $\delta_{12\nu}$ introduced earlier. The results are shown in Fig. 3. Except for the more limited range of M_N shown here, the three figures in the first column are essentially the same as in Fig. 2, as should be the case since changing the assumptions about the RHN sector do not affect the mSUGRA study. The results in the second column are, however, qualitatively different: the largest difference between the models now occurs when M_N is close to M_{GUT} . This is not difficult to understand. Since we are holding f_{ν}^2 / M_N (roughly) constant, f_{ν} is largest when M_N is large, and decreases roughly as $\sqrt{M_N}$. If $M_N \lesssim \mathcal{O}(10^{13})$ GeV, the neutrino Yukawa coupling becomes too small to have a visible effect on the sparticle masses. However, for larger values of M_N , $\delta_{LR} \propto f_{\nu}^2 \ln \frac{M_{GUT}}{M_N} \propto M_N \ln \frac{M_{GUT}}{M_N}$ grows very rapidly⁵ as long as M_N is not too close to M_{GUT} . Stau mixing then reduces the δ s shown in Fig. 3 exactly as discussed for the last figure. Once again, $\delta_{1\nu}$ offers the best separation between mSUGRA and models with a RHN, and if M_N is within a factor ~ 100 of M_{GUT} distinction between the models may be possible if sparticle masses can be measured with sufficient precision.

We find it exciting that, respecting the mass constraint, models with values of M_N close to M_{GUT} (which theoretical prejudice might suggest are the most likely) are the ones most likely to yield to experimental scrutiny. It is thus interesting to ask whether a subset of these models also satisfies the Yukawa unification condition, and if so, examine whether this “favored class” of models can be distinguished from mSUGRA. This is illustrated in Fig. 4 where we show $\delta_{1\nu}$ for (a) mSUGRA, (b) mSUGRA + RHN with $f_{\nu}(M_{GUT}) = f_t(M_{GUT})$, (c) mSUGRA + RHN with the neutrino mass constraint, and (d) mSUGRA + RHN with $f_{\nu}(M_{GUT}) = f_t(M_{GUT})$ and the neutrino mass constraint. The first three frames are the same as in previous figures and are only included for convenience. We see from frame (d) that it is indeed possible to find models where the neutrino and top Yukawa couplings unify (an $SO(10)$ -like condition) and the tau neutrino mass is in the right range. Furthermore, the bulk of these models have large values⁶ of $\delta_{1\nu}$ so that it is possible that linear collider

⁵Of course, if $M_N = M_{GUT}$ all the δ s will vanish (except for mixing effects) because there is no RG evolution. The dots in Fig. 3 terminate well before this because as M_N increases, the value of f_{ν} becomes so large that it blows up before M_{GUT} . In this case, the model is not shown.

⁶We should mention that we made a dedicated run where we generated models with sleptons lighter than 500 GeV. The results were qualitatively similar to those in frame *d*, except that the

experiments may offer a novel check of the simplest see-saw mechanism, if the relevant sparticle masses can be measured precisely enough.

Before closing this section, we briefly remind the reader that we had noted that stau mixing effects which are responsible for the few points in Fig. 4d overlapping with the mSUGRA region would be absent for the variable $3\Delta_\nu - \Delta_1 - \Delta_2$. Thus, the dimensionless version of this,

$$\delta'_{12\nu} = \frac{3\Delta_\nu - \Delta_1 - \Delta_2}{(m_{\tilde{e}_R}^2 + m_{\tilde{e}_L}^2 + m_{\tilde{\nu}_e}^2 + m_{\tilde{\tau}_1}^2 + m_{\tilde{\tau}_2}^2 + m_{\tilde{\nu}_\tau^2})/6},$$

in principle offers the hope of an even cleaner separation between the two classes of models. This is illustrated in Fig. 5 where we plot $\delta'_{12\nu}$ for (a) mSUGRA, and (b) mSUGRA + RHN model with both $f_\nu(M_{GUT}) = f_t(M_{GUT})$ and the neutrino mass constraint (9). We see a dramatic reduction in the spread for mSUGRA models in frame (a) which then resembles the first frame of Fig. 1, confirming that the spread in the other figures indeed originates from the mixing. Frame (b) shows that none of the RHN models that we generated gives $\delta'_{12\nu} < 0$, so that the separation is theoretically very clean. Of course, this measurement also requires a determination of $m_{\tilde{\tau}_2}$ and $m_{\tilde{e}_L}$ in addition to the other sparticle masses.

III. PROSPECTS FOR THIRD GENERATION SLEPTON MASS MEASUREMENTS

We have seen that a determination of $\delta_{1\nu}$ or, even better $\delta'_{12\nu}$, offers an opportunity for detecting Yukawa interactions of neutrinos, and further, for an *independent* confirmation of the simple see-saw mechanism for neutrino masses. In the simplest case where the neutrino and top Yukawa couplings unify at the GUT scale these quantities, which are zero in mSUGRA, are expected to be $\sim 0.05 - 0.2$, depending on the RHN model parameters.

Assuming that sparticles directly decay to the lightest SUSY particle (LSP) which was taken to be the lightest neutralino \tilde{Z}_1 , it has been shown [11] that masses of the first two generations of charged sleptons and charginos can be measured at the 1-1.5% level if these sparticles are within the kinematic reach of e^+e^- linear colliders. An integrated luminosity of about $50 fb^{-1}$ is sufficient to attain this precision. Longitudinal polarization of the e^- beam, which is crucial both to reduce SM backgrounds as well as to separate various SUSY processes from one another, is expected in all the current machine designs. Subsequently, it was shown [12] that this precision was not degraded even if sparticles decay via the complicated cascades [13] expected in most SUSY models. Indeed cascade decays are an asset in that they make it possible to determine, for instance, $m_{\tilde{\nu}_e}$ with a similar precision when $\tilde{\nu}_e \rightarrow \tilde{W}_1 e$ is kinematically allowed [12]. These findings have since been confirmed by more realistic studies [14,15]. Thus, whether or not $\delta_{1\nu}$ or $\delta'_{12\nu}$ can be conclusively determined to be non-zero depends mainly on the precision with which the masses of third generation

region of highest density was shifted down slightly. In particular none of the models in this new run yielded $\delta_{1\nu} > 0.2$.

charged sleptons and sneutrinos can be measured. A qualitative assessment of this forms the subject of this section.

Nojiri *et al.* [16] performed a detailed study of how well $m_{\tilde{\tau}_1}$ can be measured at a linear collider, assuming that $\tilde{\tau}_1 \rightarrow \tau \tilde{Z}_1$. Just as for the first two generations [11,12], their basic strategy for determining $m_{\tilde{\tau}_1}$ is to study the energy distribution of (hadronically decaying) daughter τ s. This study is complicated by the fact that τ is unstable and part of its energy is carried off by the undetected neutrino. As a result, the relatively sharp end-points that were obtained in earlier studies of \tilde{e}_R and $\tilde{\mu}_R$ masses are washed out. Nevertheless, assuming an integrated luminosity of 100 fb^{-1} , they are able to obtain a 1σ precision of $\sim 2\%$ on $m_{\tilde{\tau}_1}$. In their study, they confined themselves to the decay $\tau \rightarrow \rho\nu$, and estimated that by including decays to π and a_1 , they might be able to improve this by a factor of 2.

We are not aware of any studies that examine prospects for measuring $m_{\tilde{\tau}_2}$ or $m_{\tilde{\nu}_\tau}$. A systematic evaluation of this would require a dedicated study in itself, and is beyond the scope of this paper. However, in order to get some feel for whether the measurements outlined in the last section are feasible, we attempted to make a rough estimate of how well $m_{\tilde{\nu}}$ might be measured for a “typical” mSUGRA case where visible decays $\tilde{\nu} \rightarrow \tilde{W}_1 \ell$ of the sneutrino are allowed. We do not compute SM physics backgrounds (which are argued to be small) and ignore any QCD jets that may be misidentified as hadronically decaying taus. We perform only one case study and ignore bremsstrahlung and beamsstrahlung. We also assume that $m_{\tilde{W}_1}$ and $m_{\tilde{Z}_1}$ will be well measured by the time there is a large enough data sample to make it possible to consider measurements of $m_{\tilde{\nu}_\tau}$ or $m_{\tilde{\tau}_2}$, and ignore any error in these masses. Our purpose in showing these simplistic results is two-fold. First, as we said, we wanted to get a feel for whether measurements of $\delta_{1\nu}$ or $\delta'_{12\nu}$ are even feasible. Second, we found that naive extensions of methods previously used [12] for measurements of masses of heavier sleptons of the first two generations do not seem to work in this case. We felt it would be worthwhile to point this out and suggest a possible alternative.

The parameter point that we choose corresponds to an mSUGRA model with

$$m_0 = 150 \text{ GeV}, m_{1/2} = 170 \text{ GeV}, A_0 = 0, \tan\beta = 5, \mu > 0.$$

The resulting spectrum is illustrated in Table I. We see that at a $\sqrt{s} = 500 \text{ GeV}$ e^+e^- collider, all charged sleptons and sneutrinos, as well as charginos and neutralinos together with all but the charged Higgs bosons are kinematically accessible via $2 \rightarrow 2$ processes.

The production cross sections for the most important SUSY processes obtained using ISAJET [17] are shown in Fig. 6 as a function of the electron beam polarization parameter $P_L = f_L - f_R$, where f_L (f_R) is the fraction of left handed (right handed) electrons in the beam. The first item of note is that cross sections for third generation sfermions are small, and moreover, their signals are likely to suffer from contamination from production of other sparticles. Here, we begin by considering the measurement of $m_{\tilde{\tau}_1}$. Our purpose is not to improve upon the results of the detailed study of Nojiri *et al.* [16], but to see how our simplified analysis compares with their results in order to be able to assess our results for the corresponding study for $\tilde{\nu}_\tau$.

We use ISAJET v7.51 for our SUSY event simulation. We use a toy calorimeter covering $-4 < \eta < 4$ with cell size $\Delta\eta \times \Delta\phi = 0.05 \times 0.05$. Energy resolution for electrons, hadrons and muons is taken to be $\Delta E = \sqrt{.0225E + (.01E)^2}$, $\Delta E = \sqrt{.16E + (.03E)^2}$ and $\Delta p_T = 5 \times 10^{-4} p_T^2$, respectively. Jets are found using fixed cones of size $R = \sqrt{\Delta\eta^2 + \Delta\phi^2} = 0.6$

using the ISAJET routine GETJET (modified for clustering on energy rather than transverse energy). Clusters with $E > 5$ GeV and $|\eta(\text{jet})| < 2.5$ are labeled as jets. Muons and electrons are classified as isolated if they have $E > 5$ GeV, $|\eta(\ell)| < 2.5$, and the visible activity within a cone of $R = 0.5$ about the lepton direction is less than $\max(\frac{E_\ell}{10}, 1 \text{ GeV})$. Jets with $E \geq 10$ GeV and one or three charged tracks (with $p_T(\text{track}) \geq 0.5$ GeV) in a 10° cone about the jet axis, but no other tracks in a larger 30° cone, are classified as τ s if the mass of the tracks is smaller than m_τ and the total charge of the tracks is ± 1 .

A. $\tilde{\tau}_1$ mass measurement

In order to obtain a measurement of $m_{\tilde{\tau}_1}$ it is clear from Fig. 6 that it would be best to use $P_L(e^-)$ as close to -1 as possible. Then potential SUSY contamination to the $\tau\tau + \cancel{E}_T$ final state⁷ from $\tilde{W}_1\tilde{W}_1$ and $\tilde{Z}_2\tilde{Z}_2$ production, as well as from SM W^+W^- production, is minimized, resulting in a relatively clean sample of $\tilde{\tau}_1\tilde{\tau}_1$ events. We use $P_L(e^-) = -0.9$ corresponding to a 95% polarized beam. To selectively enhance the signal over SM backgrounds, we impose similar cuts used in earlier studies [11,12] of the $\tilde{\mu}_R$ signal. The difference is that instead of the dimuon final state from $\tilde{\mu}_R\tilde{\mu}_R$ production, we now have a di-tau final state in the “two narrow jets” channel. We require, (i) $E_\tau^{vis} < 200$ GeV, (ii) $E_{T\tau}^{vis} \geq 15$ GeV, (iii) $20 \text{ GeV} \leq E(\text{visible}) \leq 400$ GeV, (iv) $|\cos\theta_\tau| \leq 0.9$, (v) $-Q_\tau \cos\theta_\tau \leq 0.75$, (vi) $\theta_{acop} \leq 30^\circ$, and (vii) $\cancel{E}_T \geq 25$ GeV. We veto events with additional jets. Here, E_τ^{vis} and $E_{T\tau}^{vis}$ refer to the energy and transverse momentum of the hadronically decaying tau jet; *i.e.* the visible portion of the decay products of the tau. Cut (v) greatly reduces backgrounds from W^+W^- and also $e\nu W$ production. Unlike in the earlier study of smuon production, where an additional cut $|m_{\mu\mu} - M_Z| > 10$ GeV was imposed to eliminate backgrounds from ZZ , $\nu\nu Z$ and e^+e^-Z production, we have not imposed a mass cut on the di-tau system.

We have checked that ZZ and WW events yield a background of 0.3 fb and 0.1 fb , respectively (to be compared with the signal of $\sim 8 \text{ fb}$) and ignored $\nu\nu Z$ and e^+e^-Z backgrounds. Other SM physics sources of $\tau\tau + \cancel{E}_T$ events include $Z^* \rightarrow \tau\tau$ production, and $e^+e^- \rightarrow Z(\rightarrow \nu\nu) + h_{SM}(\rightarrow \tau\tau)$ production. The former, which (for hadronically decaying taus) has a total cross section of $\sim 200 \text{ fb}$ (before any cuts) is reduced to a negligible level after our cuts (especially (vi) and (vii)). Our simulation of this yields a cross section⁸ $\sigma \lesssim 4 \times 10^{-3} \text{ fb}$. Although we have not simulated the latter, we have run all SUSY and Higgs (including Zh) contributions for the case at hand through our cuts. We find that $\tilde{\tau}_1\tilde{\tau}_1$ production contributes 90% of the signal, and of the remaining 10%, only about 15% comes from Zh production.⁹ Since the lightest Higgs boson of the MSSM is SM-like, we infer that

⁷A τ final state always refers to the visible debris from a hadronically decaying τ .

⁸While this background may well be considerably larger than $4 \times 10^{-3} \text{ fb}$ after radiation is included, we expect that it is still negligible.

⁹About 60% of the SUSY and Higgs background comes from chargino and neutralino production (of this about 2/3 is from $\tilde{Z}_1\tilde{Z}_2$ production), and a quarter from sneutrino and stau production, with Zh making up the remainder.

the Zh_{SM} background is small. Presumably, the SUSY background can be further reduced by dedicated cuts, *e.g.* on $m_{\tau\tau}$ which has to be smaller than $m_{\tilde{Z}_2} - m_{\tilde{Z}_1}$ for di-taus from \tilde{Z}_2 decays. In the following discussion of the precision with which $m_{\tilde{\tau}_1}$ can be measured, we ignore all SUSY and SM backgrounds.

To determine $m_{\tilde{\tau}_1}$, we study the visible energy spectrum of the τ jets whose distribution is shown in Fig. 7a for the mSUGRA case under study. If the entire energy of the tau (produced via the two body decay of a scalar) could be measured, we would expect this spectrum to be flat with sharp end points in a perfect detector – the decay kinematics then determines the end points in terms of $m_{\tilde{\tau}_1}$ and $m_{\tilde{Z}_1}$ along with the beam energy. The energy spectrum in Fig. 7a is far from flat because of the energy lost to neutrinos. Since higher energy taus, on an average, lose greater energy to neutrinos, the upper end point is greatly smeared. The loss of energy to neutrinos also means that there will be signal events below the lower end point. Thus the kinematic end points do not play a role in a measurement of sparticle masses. Nevertheless, the shape and normalization of the E_τ distribution is sensitive to $m_{\tilde{\tau}_1}$.

To ascertain how well $m_{\tilde{\tau}_1}$ can be determined, we generated “theory” data samples (each with about 80 times as many stau pairs as expected for the signal case for an integrated luminosity of 100 fb^{-1}) for several values of $\tilde{\tau}_1$ mass to determine the theoretical E_τ^{vis} distribution after the cuts (the solid histogram). We also generated a synthetic “data” set for an integrated luminosity of 100 fb^{-1} (the points with error bars). Assuming that $m_{\tilde{Z}_1}$ is well determined (via a fit to the much larger sample of $\tilde{e}_R\tilde{e}_R$ and $\tilde{W}_1\tilde{W}_1$ pair events [11]) we can now fit the E_τ^{vis} distribution from the “data” to the “theory” in terms of a single parameter $m_{\tilde{\tau}_1}$. The resulting χ^2 distribution is shown in Fig. 7b. The triangles denote the actual value of χ^2 that we obtained for each theory point that we compared with. The solid curve is the best fit parabola to all these triangles. The scatter indicates the error on the theory which, as we described, was also obtained via a Monte Carlo calculation. From the figure, we obtain the fitted value of the stau mass to be $168.1 \pm 2.6 \text{ GeV}$ (1σ). In view of the scatter of our “theory”, we will be more conservative and work with the 90% CL error of $\pm 3.5 \text{ GeV}$. Our results, are not incompatible with those of Nojiri *et al.* The slightly smaller error that we get may be attributed to the fact that we have assumed that the LSP mass is known¹⁰ so that we could perform a single parameter fit, and possibly also because only $\tau \rightarrow \rho$ decays were used in their analysis.

B. $\tilde{\nu}_\tau$ mass measurement

The analysis of Ref. [12] suggests that it should be possible to measure $m_{\tilde{\nu}_\tau}$ in the same way that the electron sneutrino mass was measured. The strategy for this measurement was to focus on the sample of very clean events from the process, $e^+e^- \rightarrow \tilde{\nu}_e + \tilde{\nu}_e \rightarrow e\tilde{W}_1 + e\tilde{W}_1 \rightarrow$

¹⁰This may not seem a good assumption because the error on the stau mass is not much smaller than the expected error of $\sim 1\%$ on $m(LSP)$. We will see shortly that a much larger integrated luminosity is needed for any measurement of the mass of $\tilde{\nu}_\tau$. In this era, both the LSP and $\tilde{\tau}_1$ masses will be much better determined.

$e\mu\nu\tilde{Z}_1 + eqq\tilde{Z}_1$, where one of the charginos decays hadronically and the other leptonically. In this analysis, the electron beam was taken to be left handed. There was very little SM background or SUSY contamination to this event sample, and a two parameter fit to the flat electron energy distribution yielded $m_{\tilde{\nu}_e}$ and $m_{\tilde{W}_1}$ with a precision of just over 1% (1σ).

The same strategy suggests that we should focus on $\tau\tau\ell jj + \cancel{E}_T$ events from $\tilde{\nu}_\tau\tilde{\nu}_\tau$ production, where $\ell = e, \mu$, and study the (visible) τ energy distribution in this data sample (but, of course, change the beam polarization to be right handed to reduce backgrounds). We attempted to do so (again assuming the chargino mass will be well measured), but were unable to obtain significant discrimination between data sets with different $\tilde{\nu}_\tau$ masses. We found several factors which cause a difference from the study in Ref. [12].

1. First, $\sigma(\tilde{\nu}_e\tilde{\nu}_e)$ is much larger than $\sigma(\tilde{\nu}_\tau\tilde{\nu}_\tau)$: for our case study we see from Fig. 6 that this factor is larger than 100.
2. While the branching ratio for $\tilde{\nu} \rightarrow \ell\tilde{W}_1$ and $\tilde{W}_1 \rightarrow \ell\nu\tilde{Z}_1$ are similar (in fact the latter favours our case as we can use both e and μ decays of \tilde{W}_1), we now have to require that both taus decay hadronically (a reduction to 4/9), and further, that both the tau jets pass the identification criteria to be identified as taus.
3. Not all the energy of the tau is visible. In particular, since the visible energy of the tau is reduced due to the escaping neutrinos, we found that the energy spectrum is frequently pushed well below our tau identification threshold of 10 GeV.
4. For a left handed electron beam $\sigma(\tilde{\nu}_e\tilde{\nu}_e)$ is much larger than other SUSY cross sections, so that the event sample is very much dominated by the sneutrino signal. This is not quite the case for $\tilde{\nu}_\tau$ pair production; we see from Fig. 6 that heavier chargino and neutralino production as well as $\tilde{\tau}_2\tilde{\tau}_2$ production may make significant contributions to this event topology.

The first two items greatly reduce the number of signal events increasing the statistical error. The last item causes contamination of the sample. The energy loss due to the escaping neutrinos discussed in item (3) causes the energy distributions with different $m_{\tilde{\nu}_\tau}$ to resemble one another beyond $E_\tau = 10$ GeV more closely than they would if the full τ energy could be measured. The point is that the cut on the tau energy cuts out fewer events when the mass gap between $\tilde{\nu}_\tau$ and \tilde{W}_1 increases; *i.e.* for heavier sneutrinos, assuming as we do that the chargino mass is fixed. But the sneutrino production cross section reduces for larger sneutrino mass. As a result, these two effects compensate, reducing the discrimination between different sneutrino mass cases.¹¹ We also examined other decay chains (with just one identified τ) but found that these generally suffered from large contamination from other SUSY sources. We conclude that this strategy is not suitable for such a measurement even with an integrated luminosity of 500-1000 fb^{-1} .

¹¹Of course, at the high energy end the spectra are sensitive to the sneutrino mass, but there we do not have sufficient event rate to significantly contribute to χ^2 in an analysis similar to the one for $m_{\tilde{\tau}_1}$ determination discussed above.

The energy dependence of the cross section provides an alternative way to measure the sneutrino mass. Since we have not taken bremsstrahlung or beamsstrahlung into account, we are careful not to go very close to the kinematic threshold where the cross section would be most strongly affected by soft photon emission. Away from the threshold, we expect that beamsstrahlung effects may reduce the cross section by $\sim 10\%$, but presumably without greatly altering its energy dependence.

The total cross section for $\tau\tau\ell jj + \cancel{E}_T$ events from all SUSY sources is shown in Fig. 8a for the signal point with $m_{\tilde{\nu}_\tau} = 178.1$ GeV, as well as for two other values of the sneutrino mass. Here, we have required that each τ jet has $E_\tau^{vis} \geq 10$ GeV. We also require $\cancel{E}_T \geq 25$ GeV. SM physics backgrounds are expected to be small. The error bars correspond to an integrated luminosity of 200 fb^{-1} for each energy. For the contamination from SUSY events, we have added contributions from other SUSY sources but with mSUGRA parameters fixed to their case study values¹² regardless of $m_{\tilde{\nu}_\tau}$.

The cross section for sneutrino events, along with that for the other important contributors to this topology, is shown in Table II for the energy range in Fig. 8. We see that the contribution from $\tilde{\tau}_2\tilde{\tau}_2$ production is always much smaller than that from charginos and neutralinos. For this case, the SUSY backgrounds are smaller than or comparable to the signal for $\sqrt{s} \lesssim 550$ GeV, but for larger values of \sqrt{s} the heavy chargino and neutralino contributions overwhelm the sneutrino signal. The sharp increase in the cross section from charginos and neutralinos that is seen for $\sqrt{s} \geq 550$ GeV is due to the opening up of heavy neutralino and chargino pair production thresholds.

To get an idea of how well cross sections can distinguish different sneutrino masses, we perform a Monte Carlo computation of the cross section for several values of sneutrino mass for energies ranging between 425 GeV and 600 GeV in steps of 25 GeV. We generate about 10^5 SUSY events which is about 30 times the number of signal events expected for an integrated luminosity of 200 fb^{-1} . For each value of $m_{\tilde{\nu}_\tau}$ that we consider, we then compute $\Delta\chi^2$ between the energy dependence of the cross section for the case study point and the corresponding quantity for some other $\tilde{\nu}_\tau$ mass. Our results are shown in Fig. 8b for a statistical error bar corresponding to an integrated luminosity of 100 fb^{-1} per point (circles) and 200 fb^{-1} per point (triangles). Also shown is the line corresponding to $\Delta\chi^2 = 2.7$ (the 90% CL in the Gaussian limit). The solid (dashed) curves are a fit through the circles (triangles). Using these fits, we see that the sneutrino mass is obtained as $m_{\tilde{\nu}_\tau} = 178_{-18}^{+15}$ GeV ($m_{\tilde{\nu}_\tau} = 178_{-13}^{+10}$ GeV) for an integrated luminosity of 100 fb^{-1} (200 fb^{-1})

¹²This is a conservative attitude, because if we compute the SUSY background (mainly from heavier chargino and neutralino production at the highest energies) using the different mSUGRA parameters for each sneutrino mass case, the *SUSY background cross sections* change enough to allow a discrimination between the scenarios. This occurs because of the change in chargino and neutralino masses, but these will be well determined by the time tau sneutrino mass determination might become possible. Our assumption is, perhaps, ultra-conservative in that effects from a change in the sneutrino mass, which also change the branching fractions of charginos and neutralinos, are ignored.

at the 90% CL.¹³ We recognize that even with an integrated luminosity of 100 fb^{-1} per point, it would take several years of running to obtain the 800 fb^{-1} of integrated luminosity that would be needed, assuming current projections for the anticipated luminosity of such a machine. It is worth keeping in mind that new developments (*e.g.* vertex detection, neural net algorithms, or something else) will, quite possibly, result in a significantly higher efficiency for tau identification than assumed in our analysis. In this case, the integrated luminosity required will be correspondingly reduced. Our purpose, however, is not to imply that $\tilde{\nu}_\tau$ mass measurement is possible, but to clarify just how challenging such a measurement might be.

The analysis above assumes that it would not be possible to sort out chargino and neutralino events from $\tilde{\nu}_\tau$ events. Since the heavier chargino \tilde{W}_2 and the heavier neutralinos $\tilde{Z}_{3,4}$ dominantly decay to real W , Z or h and light charginos and neutralinos, it might be conceivable that by the time such large data samples become available, experimentalists might have learnt to recognize (the bulk of) \tilde{W}_1 and \tilde{Z}_2 , in the same way that they recognize b -jets and τ -leptons today. Alternatively, although the case study point allows for heavy chargino and neutralino production, it could be that for another point, SUSY contamination from these sources is kinematically suppressed. In either case, the chargino and neutralino sample would then not contaminate the sneutrino sample. To see how much this would improve the sneutrino mass measurement, we have redone the analysis in Fig. 8, but assumed that there is no background in the $\tau\tau\ell jj$ channel.¹⁴ Our results are shown in Fig. 9 where we have taken the integrated luminosity to be 100 fb^{-1} per point. As before, the upper frame shows the cross section and the lower one $\Delta\chi^2$, defined the same way as in Fig. 8. We see from frame (a) that measurements at the lower energy can readily distinguish very heavy sneutrinos, as their production is kinematically suppressed. But these measurements do not give as sharp a distinction for sneutrinos lighter than the test case.¹⁵ For this case then, measurements at the high energy end improve the discrimination. This is manifested in Fig. 9b where we show $\Delta\chi^2$ for a scan of 425-550 GeV for which the signal exceeds the SUSY background (triangles), and also after including the highest two energy points (circles) keeping in mind that the sneutrino sample is then highly contaminated. Indeed, we see that the two curves match at the high mass end, but including the 575 and 600 GeV bins significantly improves the discrimination for lower values of $m_{\tilde{\nu}}$. We see that if SUSY backgrounds can be controlled, a sneutrino mass measurement of comparable precision as in Fig. 8 might be possible with half the integrated luminosity.

We conclude that a precise determination of $m_{\tilde{\nu}_\tau}$ poses a formidable challenge. Naively

¹³The $\Delta\chi^2$ distribution is not exactly symmetric, so that one should not view the 90% CL literally, but regard the result as a qualitative indicator of the precision of the measurement.

¹⁴This is of course overly optimistic because $\tilde{\tau}_2\tilde{\tau}_2$ events would be kinematically similar to sneutrino events. Also, \tilde{Z}_4 and \tilde{W}_2 have a branching fraction of $\sim 3\%$ to decay into $\tilde{\nu}_\tau$.

¹⁵ We could go to yet lower energy, but we constrained ourselves to stay away from the threshold. Of course, if backgrounds can be really eliminated, or reliably subtracted, an energy scan close to the sneutrino threshold might yield the maximum precision.

following the ideas in Ref. [12] that worked so well for a measurement of $m_{\tilde{\nu}_e}$ simply does not work. It appears possible that the energy dependence of the cross section for $\tau\tau\ell jj + \cancel{E}_T$ events might allow a mass measurement at the 8-10% level, but such measurements would take several years with current projections for the integrated luminosity. With a data sample of 1600 fb^{-1} distributed over 8 energy points a 6-7% measurement appears possible. Alternatively, if we can distinguish chargino/neutralino from sneutrino initiated events without substantial loss of signal, a similar precision might be possible with just half this luminosity. We should remember that we are conservatively quoting 90% CL and not 1σ errors, partly because of the simplified way that we have done our calculation.

We have not attempted to do an analysis of a measurement of $m_{\tilde{\tau}_2}$ which decays via $\tilde{\tau}_2 \rightarrow \tau\tilde{Z}_1$ (10%), $\tau\tilde{Z}_2$ (37%) and $\nu\tilde{W}_1$ (53%). The dominant decays lead to $\tilde{W}_1\tilde{W}_1 + \cancel{E}_T$ events which have a large contamination from $\tilde{W}_1\tilde{W}_1$ production. This could be reduced by using a right handed electron beam, but even for 95% polarization, the cross section from direct chargino production exceeds that for chargino production via heavy stau pair production a factor of about 3. Moreover, other SUSY sources ($\tilde{Z}_2\tilde{Z}_2$, $\tilde{W}_1\tilde{W}_2$ and even $\tilde{\nu}_\tau\tilde{\nu}_\tau$ production) could contaminate the signal especially from hadronic decays of daughter charginos. While it is possible that a clever use of the other decays modes of $\tilde{\tau}_2$ may well allow a measurement of its mass, we believe that this poses an even greater challenge than the measurement of the $\tilde{\nu}_\tau$ mass.

IV. CAN SLEPTON MASSES PROBE RIGHT HANDED NEUTRINO COUPLINGS?

We saw in Sec. II that the variables $\delta_{1\nu}$ and $\delta'_{12\nu}$ offer the best hope for measuring effects of the sneutrino Yukawa coupling. While the latter is theoretically cleaner in that models with and without a RHN are better separated, its determination requires a measurement of $m_{\tilde{\tau}_2}$ in addition to $\tilde{\tau}_1$, $\tilde{\nu}_\tau$ and other slepton masses. Since we have just explained the difficulties associated with this measurement, we will focus on the prospects for the determination of just $\delta_{1\nu}$ in the remainder of this paper. Within the simplest see-saw model with unified top and ν_τ Yukawa couplings at M_{GUT} , Fig. 4d shows that a large fraction of RHN models have $\delta_{1\nu} \gtrsim 0.1$. The question then is whether experiments at linear colliders will have the sensitivity to distinguish $\delta_{1\nu} = 0$ from $\delta_{1\nu} \gtrsim 0.1$.

It is straightforward to check¹⁶ that if the error in measuring first generation masses is negligible and mass differences between the various sleptons are small, the error in $\delta_{1\nu}$ is given by

$$(\Delta\delta_{1\nu})^2 = 16 \left(\frac{\Delta m_{\nu_\tau}}{m_{\nu_\tau}} \right)^2 + \left(\frac{\Delta m_{\tilde{\tau}_1}}{m_{\tilde{\tau}_1}} \right)^2. \quad (10)$$

Even neglecting the error in the measurement of $m_{\tilde{\tau}_1}$, it appears that m_{ν_τ} needs to be determined at about the 2.5% level in order to obtain the required precision on $\delta_{1\nu}$. Unfortunately,

¹⁶The variance of a function $f(x_1, x_2, \dots, x_n)$ of the uncorrelated quantities x_i is $\sum \left(\frac{\partial f}{\partial x_i} \right)^2 (\Delta x_i)^2$, where the derivative is evaluated at the mean value of x_i , and $(\Delta x_i)^2$ is the variance of x_i .

in view of the analysis in the previous section this does not seem to be possible, at least using the techniques considered in this study. Even if we change the 90% CL error bar to the “ 1σ ” error bar ($\Delta\chi = 1$) the error on $m_{\tilde{\nu}_\tau}$ seems to be about 4%. It thus appears to us that the effects of the tau neutrino Yukawa coupling on sparticle masses seems to be beyond the projected sensitivity of linear collider experiments, at least within the framework of the simplest GUT model with unification of neutrino and top Yukawa couplings. However, if we allow the neutrino Yukawa coupling at the GUT scale to be somewhat larger than f_t (but still require f_ν not to blow up before M_{GUT}) then linear collider experiments could be sensitive to the presence of the RHN as can be seen from Fig. 3b.

In obtaining this conclusion, we assumed that the only information we would have is on the masses of various sleptons. It could, however, be that a measurement of $\tan\beta$ may also be possible [11,8]. In this case, we would not need to combine the masses to eliminate the ($\tan\beta$ -dependent) effects of the usual tau Yukawa coupling so that, in principle, a direct measurement of stau and $\tilde{\nu}_\tau$ masses would contain information about f_ν . We checked that in all the models we generated that satisfied the Super-Kamiokande neutrino mass constraint *and* had $f_t = f_\nu$ at the unification scale, *i.e.* the models in frame (d) of Fig. 4, $m_{\tilde{\nu}_\tau}$ and $m_{\tilde{\tau}_2}$ differ from their mSUGRA values by less than 7% (typically 3-5%) while $m_{\tilde{\tau}_1}$ almost always differs by less than 3% (since $\tilde{\tau}_1 \sim \tilde{\tau}_R$, we expect it to be less affected by f_ν). We thus conclude that even in this case, it would be very difficult to discern the effect of the neutrino Yukawa coupling, except maybe for a small sub-set of model parameters.

This pessimistic outlook hinges upon the assumption of the simplest see-saw model. It is, however, worth keeping in mind that there are other models for neutrino masses that have been suggested. For instance, in a model [18] with an additional $SO(10)$ singlet with mass M_S in the superpotential, and a GUT Higgs sector comprising of just **16** dimensional representations, the light neutrino mass would take the form $m_\nu = M_S m_t^2 / M_N^2$, so that neutrino masses are still hierarchical but depending on M_S , M_N would be considerably smaller than in the case of the usual see-saw.¹⁷ In the extreme case [20] where $M_S \sim 1 \text{ TeV}$, the RHN could be as light as 10^8 GeV . In this case, we see from Fig. 4c that $\delta_{1\nu} = 0.2 - 0.5$ which is in the range that experiments at linear colliders should be sensitive to.

We also looked at the analysis [21] of neutrino masses within the framework of a localized gravity model with non-factorizable geometry, where it was shown that neutrino masses were given by $m_{\nu_i} \sim M \times (\frac{v}{M})^{r_i+1/2}$. Here, the compactification scale $M \sim M_{Planck}$, v is the electroweak vev and r_i a real number $\geq 1/2$. For $r_i = 3/2$, this reduces to the familiar see-

¹⁷This mechanism has been dubbed the type III see-saw, with the usual see-saw mechanism being the type I see-saw. In this context, we remark that for the type II see-saw [19] we have the usual 2×2 neutrino mass matrix, but with an induced non-zero Majorana mass m_L for the left handed neutrino which contributes additively to the physical light neutrino mass. This new contribution could be independent of the usual Yukawa couplings, and so may be generation-independent, giving (approximately) degenerate neutrinos of mass m when $m \gg m_{u,c}^2 / M_N$. The splitting between neutrinos is still about m_t^2 / M_N so that Δm^2 measured in neutrino oscillation experiments is now $\sim 2mm_t^2 / M_N$, which requires even larger M_N than the usual see-saw to satisfy the Super-Kamiokande measurement. Thus with the type II see-saw, we do not expect to see measurable effects in the slepton sector.

saw-like formula. One might, at first glance, think that by adjusting r_i it would be possible to allow smaller values of M which could then be probed via slepton masses. This is not the case because in this framework lepton number is conserved, and neutrinos only get a Dirac mass. In other words, the induced neutrino Yukawa coupling is tiny, essentially because of the small overlap between the active left handed neutrino (which is confined to the brane) and the sterile neutrino in the bulk. We thus expect slepton masses to be unchanged from their mSUGRA values in such a scenario.

In summary, we examined the effects of neutrino Yukawa couplings on the masses of sleptons and sneutrinos present in supersymmetric models. For most of the analysis, we assumed the simplest see-saw model for neutrino masses, and also worked within the SUSY GUT framework which implies a hierarchy of neutrino masses. Assuming that third generation neutrinos are the heaviest, we then expect the largest effect amongst third generation sleptons. To separate the effect of the MSSM tau Yukawa coupling from the new neutrino Yukawa coupling, we constructed several combinations of masses, which are expected to be zero in the mSUGRA model but deviate from this in the RHN framework. Our results are shown in Fig. 2 as a function of the RHN mass scale M_N , assuming that the top and neutrino Yukawa couplings unify at the GUT scale. The Super-Kamiokande atmospheric neutrino data, interpreted as neutrino oscillations, however, implies that m_{ν_τ} is between 0.033 and 0.1 eV. In this case M_N cannot be too far from M_{GUT} . The best discrimination is obtained via the variables $\delta_{1\nu}$ and $\delta'_{12\nu}$. Fig. 4d and Fig. 5b show that experiments should be sensitive to the difference between 0 and about 0.06-0.1 in order to conclusively discriminate RHN models from mSUGRA. Toward this end, we did a simplified analysis of the precision with which third generation sparticle masses might be measured at future e^+e^- colliders. While we confirmed the conclusions of previous analyses that $\tilde{\tau}_1$ could be measured with a precision of $\sim 2\%$, we found that with the techniques that we examined $m_{\tilde{\nu}_\tau}$ could at best be measured with a precision of $\sim 6 - 8\%$, even with optimistic projections for the luminosity and what might be achievable in the future. This then led us to conclude that such mass measurements would not be able to discriminate models with a RHN from mSUGRA within this simple framework. We saw however, that if we give up the unification of top and neutrino Yukawa couplings, or allow a more complicated framework (the type III see-saw) such a discrimination might be possible.

We conclude that precision measurements of charged slepton and sneutrino masses can provide information about RHN masses and couplings. For instance, a non-vanishing value of $\delta_{1\nu}$ (or $\delta'_{12\nu}$) would provide strong confirmation of large Yukawa interactions of neutrinos, and hence an underlying GUT scale see-saw type mechanism. This would then eliminate whole classes of alternatives including: (i) neutrino masses have Majorana type contributions only, (ii) neutrino masses are purely Dirac with Yukawa couplings strongly suppressed for symmetry [22] or geometric [21] reasons, or (iii) there might be a TeV scale¹⁸ see-saw, again with very suppressed (effective) Yukawa interactions of neutrinos [22]: in all these cases, we would expect that $\delta_{1\nu} = \delta_{12\nu} \simeq 0$.

¹⁸Within this framework, right handed neutrinos and sneutrinos are at the TeV scale. The presence of a weak scale $\tilde{\nu}_R$ can result in very different sneutrino phenomenology which might be probed at colliders, or via its cosmological implications [22].

While much attention has been focussed on measurements of charginos, neutralinos, and first generation sparticle masses, there have been few studies for the third generation of sfermions. On the other hand, it is just these masses (not only sleptons and sneutrinos, but also squarks) which are frequently sensitive to new physics at the high scale (especially physics associated with family structure). This study exemplifies the need to develop new techniques to measure third generation sparticle properties more precisely.

ACKNOWLEDGMENTS

We are grateful to M. Nojiri, S. Pakvasa and M. Peters for discussions. This research was supported in part by the U. S. Department of Energy under contract number DE-FG02-97ER41022 and DE-FG-03-94ER40833.

REFERENCES

- [1] For recent reviews, see *e.g.* S. Martin, in *Perspectives on Supersymmetry*, edited by G. Kane (World Scientific), hep-ph/9709356; M. Drees, hep-ph/9611409 (1996); J. Bagger, hep-ph/9604232 (1996); X. Tata, *Proc. IX J. Swieca Summer School*, J. Barata, A. Malbousson and S. Novaes, Eds. hep-ph/9706307; S. Dawson, Proc. TASI 97, J. Bagger, Ed. hep-ph/9712464.
- [2] K. Inoue, A. Kakuto, H. Komatsu and H. Takeshita, *Prog. Theor. Phys.* **68**, 927 (1982) and **71**, 413 (1984).
- [3] Y. Fukuda *et al.*, *Phys. Rev. Lett.* **82**, 2644 (1999); S. Fukuda *et al.* hep-ex/0009001 (2000).
- [4] M. Gell-Mann, P. Ramond and R. Slansky, in *Supergravity, Proceedings of the Workshop*, Stony Brook, NY 1979 (North-Holland, Amsterdam); T. Yanagida, KEK Report No. 79-18, (1979).
- [5] See *e.g.* M. K. Parida and N. Nimai Singh, *Phys. Rev.* **D59**, 032002 (1999).
- [6] For the impact of the RHN on other aspects of SUSY phenomenology see, J. Hisano, T. Moroi, K. Tobe, M. Yamaguchi and T. Yanagida, *Phys. Lett.* **B357**, 579 (1995); J. Hisano, T. Moroi, K. Tobe and M. Yamaguchi, *Phys. Rev.* **D53** (1996); J. Hisano and D. Nomura, *Phys. Rev.* **D59**, 116005 (1999); T. Moroi, *JHEP* **03**, 019 (2000); K. Babu, B. Dutta and R.N. Mohapatra, hep-ph/0006329 (2000).
- [7] T. Moroi, *Phys. Lett.* **B321**, 56 (1994).
- [8] V. Barger, T. Han and J. Jiang, hep-ph/0006223 (2000).
- [9] We use the renormalization group equations as given in H. Baer, M. Díaz, P. Quintana and X. Tata, *JHEP* **04**, 016 (2000). See also J. Hisano *et al.* Ref. [6].
- [10] S. Martin and M. Vaughn, *Phys. Rev.* **D53**, 3871 (1996); explicit 2-loop renormalization group equations for the MSSM plus a RHN are given in H. Baer *et al.* (paper in preparation).
- [11] T. Tsukamoto *et al.*, *Phys. Rev.* **D51**, 3153 (1995).
- [12] H. Baer, R. Munroe and X. Tata, *Phys. Rev.* **D54**, 6735 (1996).
- [13] H. Baer, A. Bartl, D. Karatas, W. Majerotto and X. Tata, *Int. J. Mod. Phys.* **A4**, 4111 (1989).
- [14] M. Danielson *et al.* in *New Directions for High Energy Physics*, Snowmass 96 Summer Study, D. Cassel, L. Trindle Gennari and R.H Siemann, Editors (1997).
- [15] S. Kuhlman *et al.* NLC Zero Design Report, SLAC Report 485 (1996).
- [16] M. Nojiri, K. Fujii, and T. Tsukamoto, *Phys. Rev.* **D54**, 6756 (1996).
- [17] F. Paige, S. Protopopescu, H. Baer and X. Tata, hep-ph/0001086 (2000).
- [18] R. N. Mohapatra and J.W.F. Valle, *Phys. Rev.* **D34**, 1642 (1986).
- [19] For a review, see R. N. Mohapatra, hep-ph/9910365 (1999).
- [20] This extreme case for the neutrino mass matrix is also realized in the flipped $SU(5)$ model as discussed by M. Drees and X. Tata, *Phys. Lett.* **B206**, 259 (1988).
- [21] Y. Grossman and M. Neubert, *Phys. Lett.* **B474**, 361 (2000).
- [22] N. Arkani-Hamed, L. Hall, H. Murayama, D. Smith and N. Weiner, hep-ph/0006312 (2000).

TABLES

TABLE I. Sparticle masses for the mSUGRA case study of Sec. III. Squarks are not accessible for the entire range of energies that we consider, except for stop; $m_{\tilde{t}_1} = 274.7$ GeV so that its pair production would be accessible for $\sqrt{s} \geq 550$ GeV. Second generation slepton masses are the same as those of the first generation.

particle	m (GeV)	particle	m (GeV)	particle	m (GeV)
\tilde{e}_R	167.8	\tilde{Z}_1	59.9	h	105.0
\tilde{e}_L	194.2	\tilde{Z}_2	108.2	H	312.6
$\tilde{\nu}_e$	178.3	\tilde{Z}_3	255.5	A	310.4
$\tilde{\tau}_1$	165.7	\tilde{Z}_4	284.3	H^\pm	320.4
$\tilde{\tau}_2$	195.4	\tilde{W}_1	105.6	\tilde{u}_L	397.5
$\tilde{\nu}_\tau$	178.1	\tilde{W}_2	283.4	\tilde{g}	427.8

TABLE II. Cross sections in fb for the $\tau\tau\ell jj$ signal from $\tilde{\nu}_\tau\tilde{\nu}_\tau$ production for the case study of Sec. III, as a function of the center of mass energy \sqrt{s} after the cuts described in the text. Also shown are the corresponding cross sections from $\tilde{\tau}_2\tilde{\tau}_2$ production, and from chargino and neutralino production. As discussed in the text, the cross sections in the last two columns have been used as the background for *all* sneutrino masses in Fig. 8.

\sqrt{s} (GeV)	$\sigma(\tilde{\nu}_\tau\tilde{\nu}_\tau)$ (fb)	$\sigma(\tilde{\tau}_2\tilde{\tau}_2)$ (fb)	$\sigma(\tilde{W}_i\tilde{W}_j, \tilde{Z}_i\tilde{Z}_j)$ (fb)
425	0.083	0.008	0.053
450	0.116	0.015	0.071
475	0.140	0.019	0.078
500	0.139	0.028	0.079
525	0.149	0.029	0.078
550	0.149	0.036	0.127
575	0.145	0.032	0.219
600	0.134	0.037	0.270

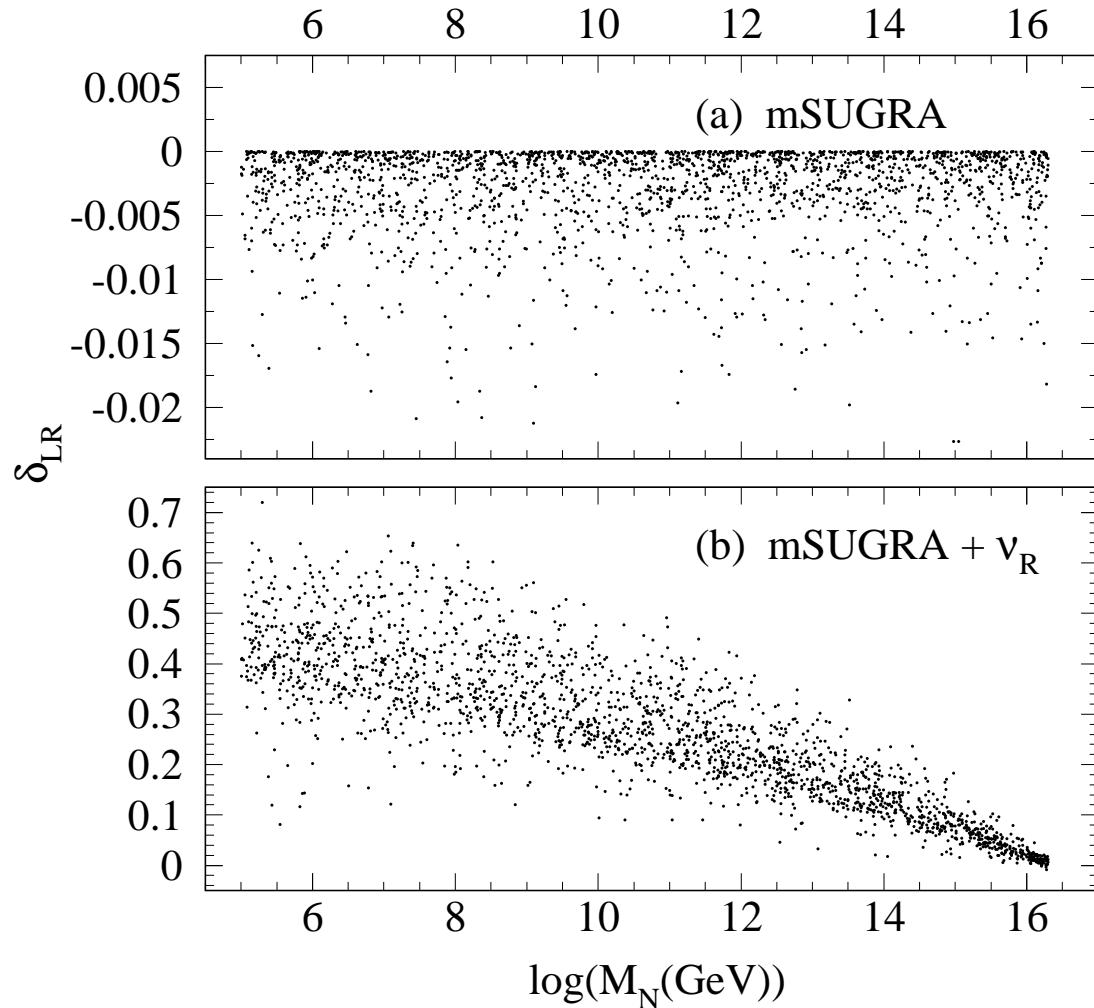


FIG. 1. The distribution of δ_{LR} , defined in the text, for a set of randomly generated (a) mSUGRA models, and (b) models with a right handed neutrino, versus the ν_R mass M_N . In case (a) M_N is randomly assigned. We assume that the top and neutrino Yukawa couplings unify at the GUT scale.

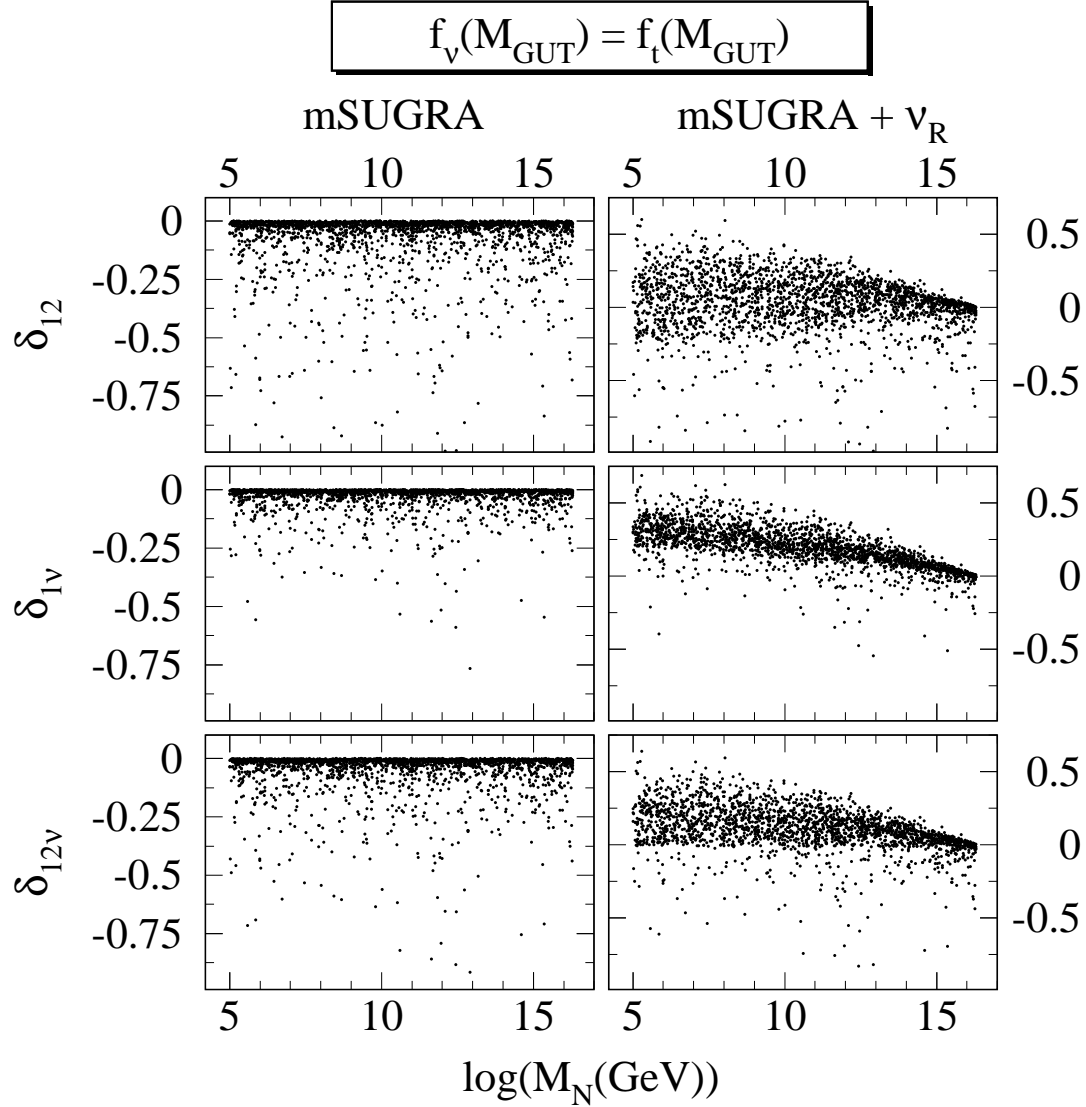


FIG. 2. The distribution of the quantities δ_{12} (first row), $\delta_{1\nu}$ (second row) and $\delta_{12\nu}$, defined in Sec. II of the text, for the same set of models as in Fig. 1 versus M_N . The first column shows the results for mSUGRA models, and the second one shows the corresponding results for models with a ν_R . We assume that the top and neutrino Yukawa couplings unify at the GUT scale.

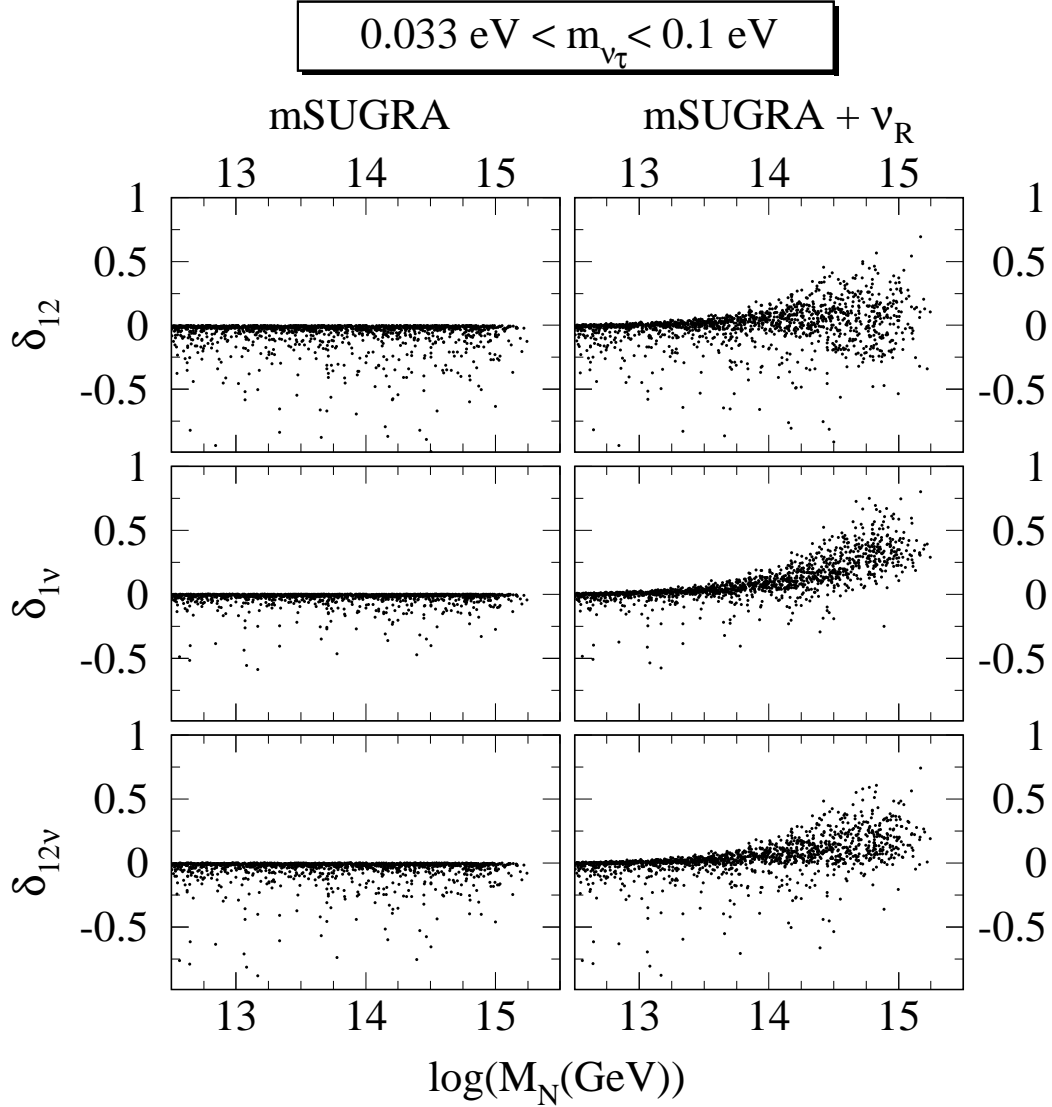


FIG. 3. The same as Fig. 2 except that instead of assuming that the Yukawa couplings unify at the GUT scale, we require that the mass of the tau neutrino is between the Super-Kamiokande range of 0.033 eV and 0.1 eV.

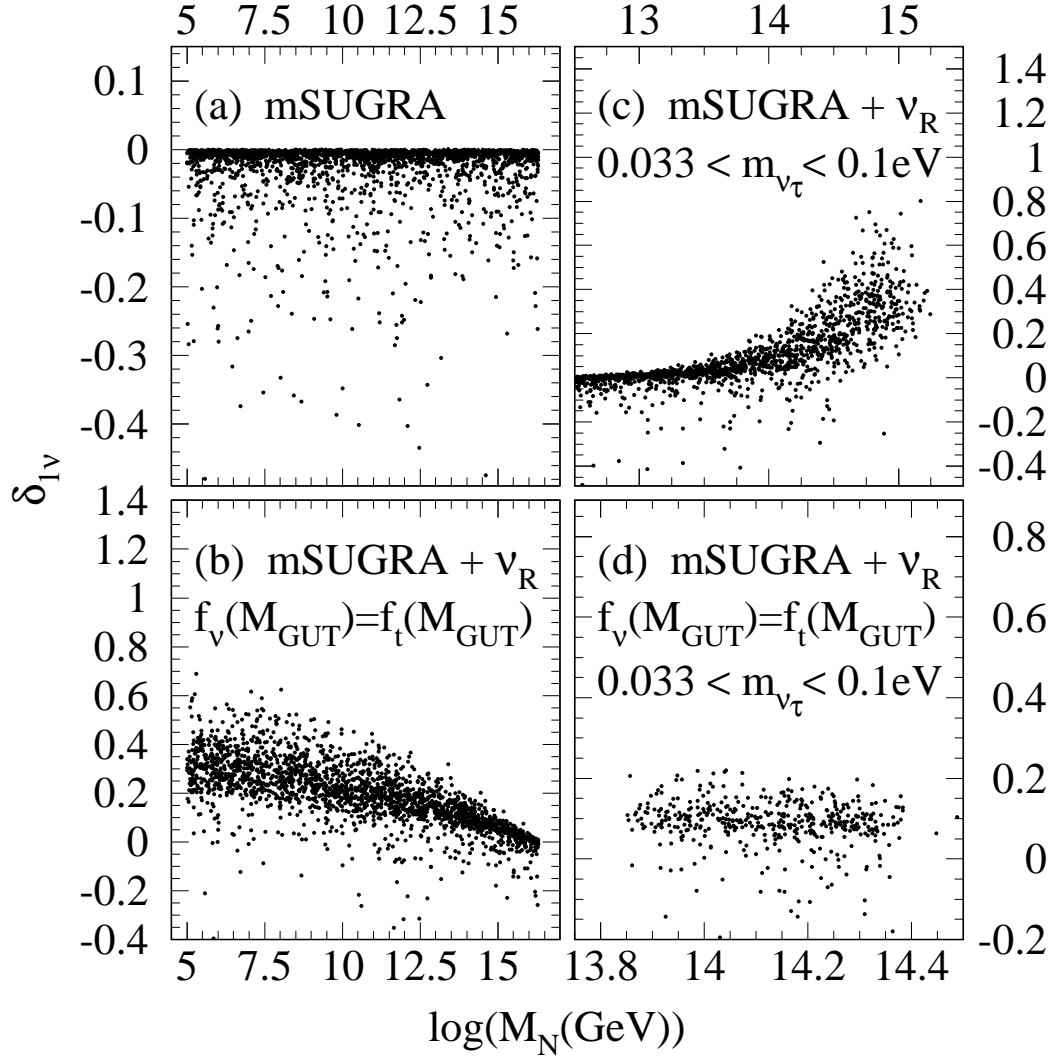


FIG. 4. The distribution of $\delta_{1\nu}$ versus the right handed neutrino mass M_N for the (a) mSUGRA model, (b) the RHN model with unification of top and neutrino Yukawa couplings, (c) the RHN model with the ν_τ mass in the Super-Kamiokande range, and (d) the RHN model with $f_t = f_{\nu_\tau}$ at the GUT scale and the Super-Kamiokande constraint on m_{ν_τ} . Notice the difference in the horizontal scales for the two columns.

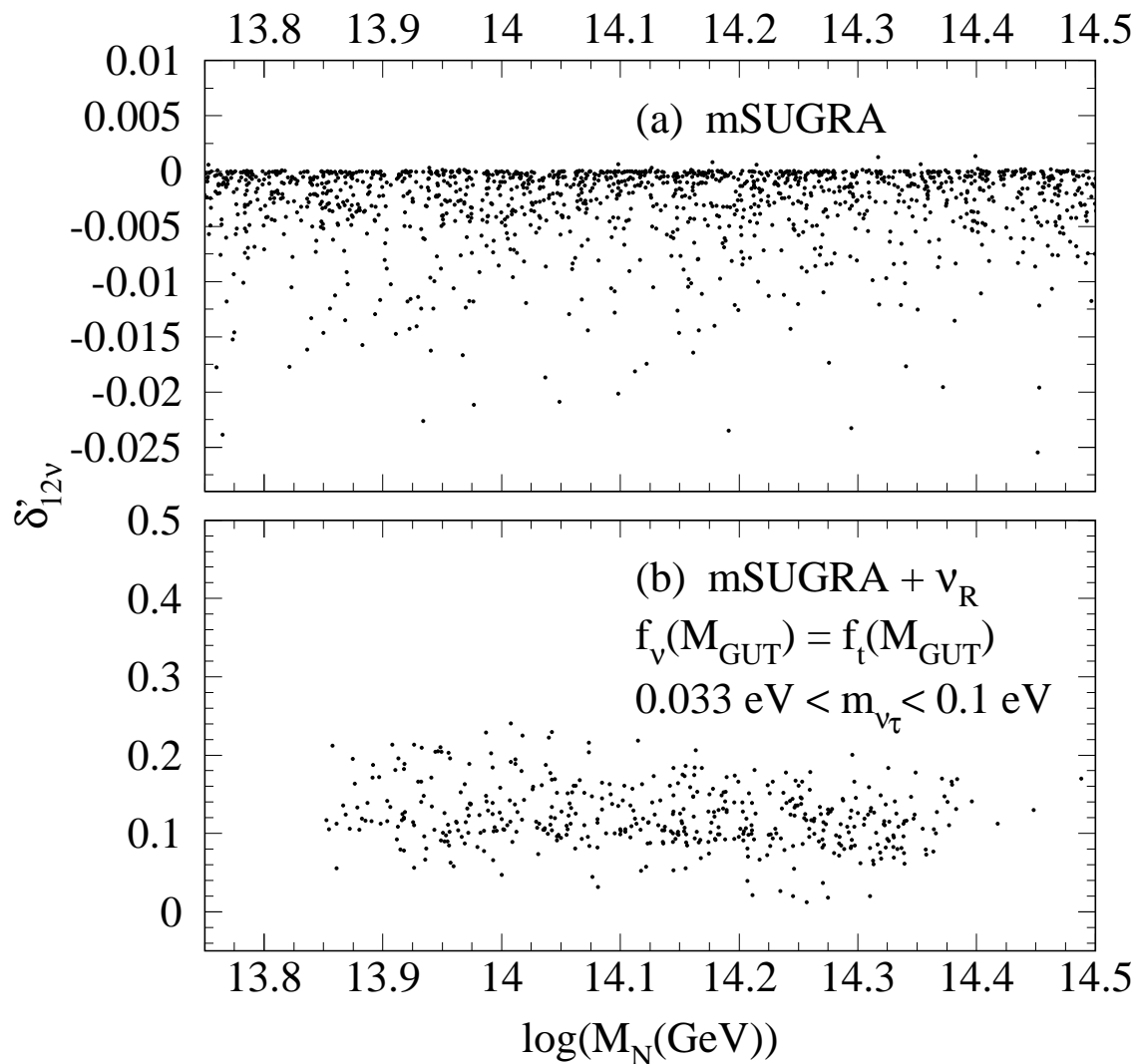


FIG. 5. The distribution of $\delta'_{12\nu}$ defined in the text versus M_N for the (a) mSUGRA model, and (b) the RHN model with $f_t = f_{\nu_\tau}$ at the GUT scale and the Super-Kamiokande constraint on m_{ν_τ} .

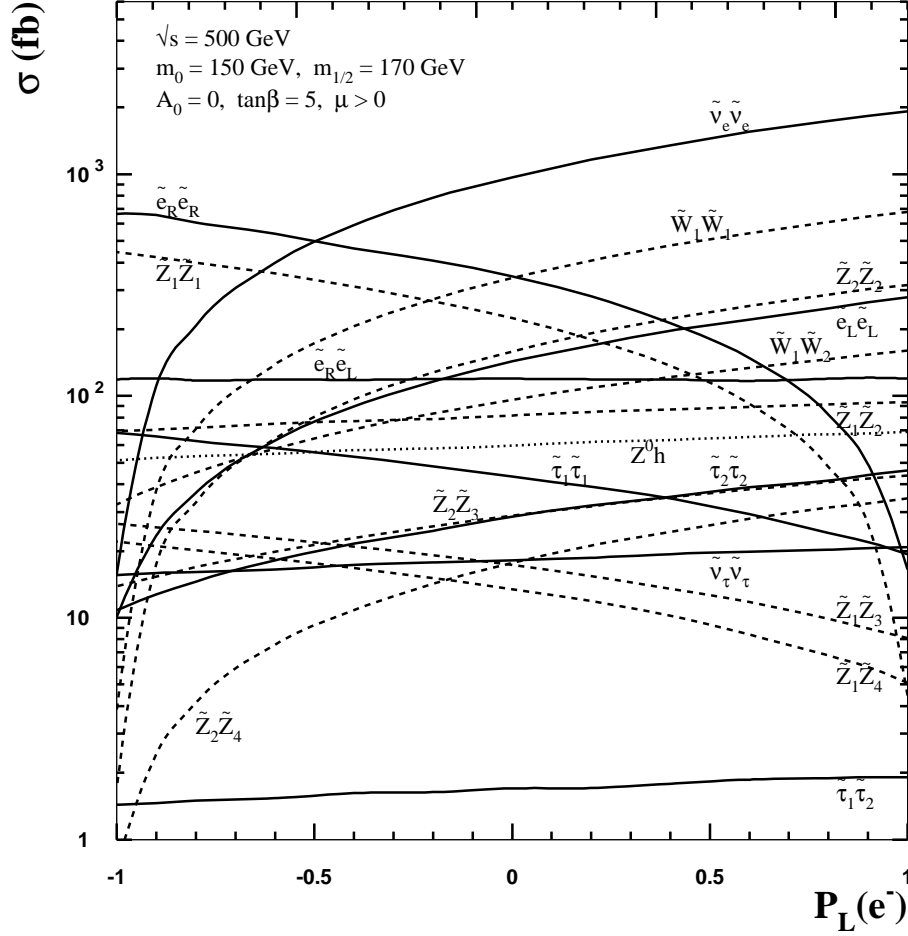


FIG. 6. Cross sections for various SUSY production processes at an e^+e^- collider with $\sqrt{s} = 500 \text{ GeV}$ versus the electron beam polarization parameter $P_L(e^-)$ for the case study in Sec. III. The solid lines show cross sections for sleptons, the dashed lines for charginos and neutralinos and the dotted lines for Higgs boson production mechanisms. The cross sections for Ah and ZH production are below the 1 fb level.

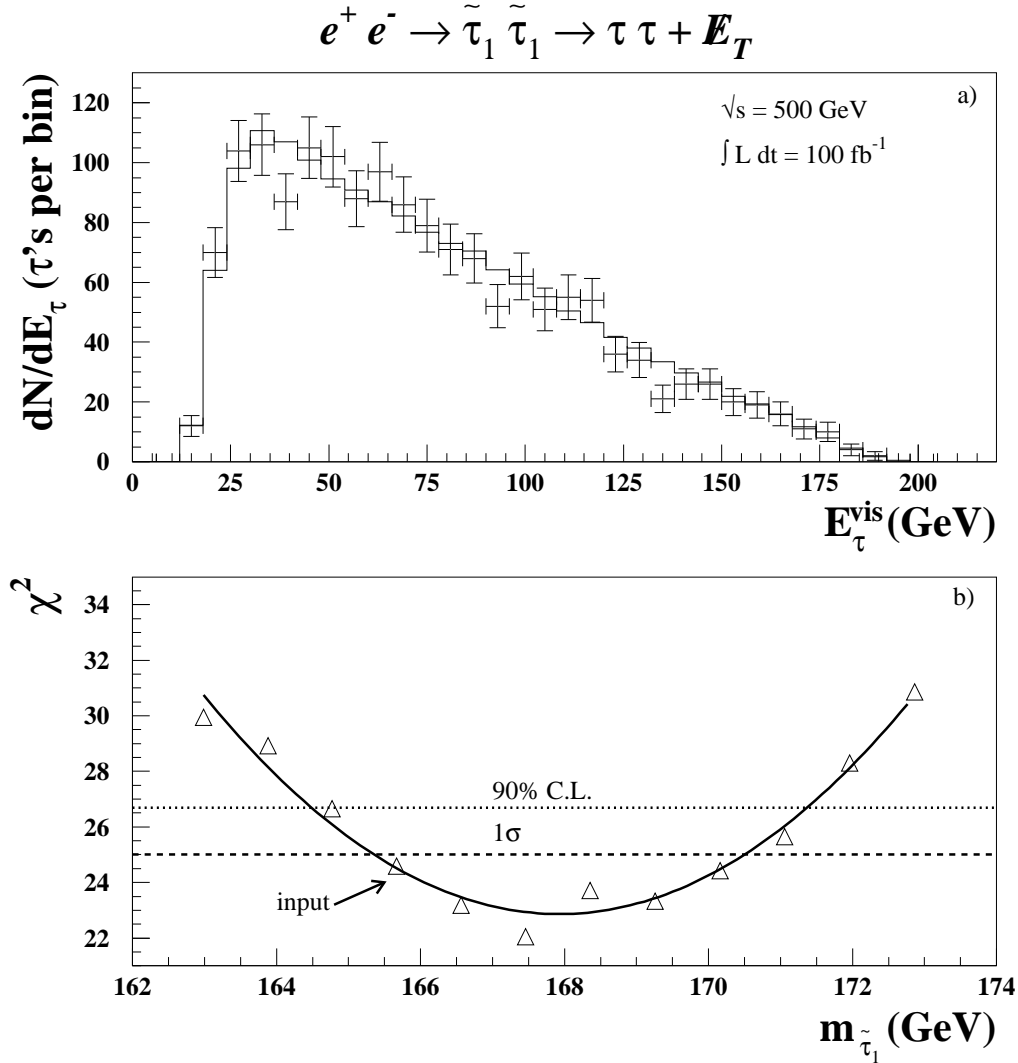


FIG. 7. (a) The distribution of the visible energy from the hadronic decays of taus produced via $e^+e^- \rightarrow \tilde{\tau}_1\tilde{\tau}_1 \rightarrow \tau\tau + \cancel{E}_T$ events at a 500 GeV collider for the case study of Sec. III. The solid histogram denotes the theoretical expectation after cuts, while the points are the synthetic data for an integrated luminosity of 100 fb^{-1} . Note that each event contributes two visible taus. In (b), the values of χ^2 obtained by a comparison of synthetic data for several values of $m_{\tilde{\tau}_1}$ with the theory histogram in (a) above are shown by the triangles. The line is the best-fit parabola through the triangles. The case study point is shown denoted as input, and the dashed and dotted lines denote the 1σ and 90% confidence levels for stau mass measurement. The integrated luminosity is taken to be 100 fb^{-1} .

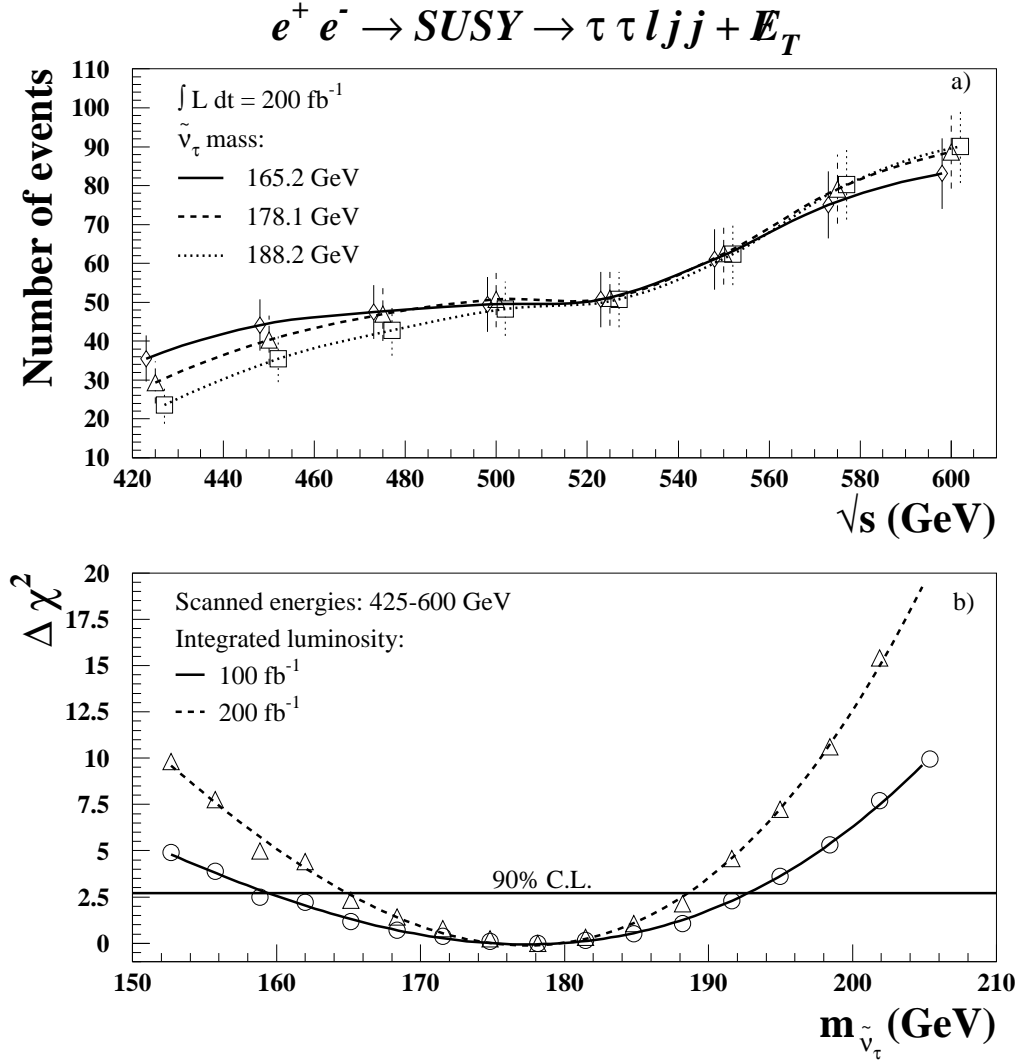


FIG. 8. (a) The cross section after cuts described in the text for $\tau\tau l j j + \cancel{E}_T$ events from all SUSY processes (however, see the text for a discussion of how SUSY backgrounds are computed) for the case study point (dashed) and two other points with a lighter (solid) and heavier (dotted) tau sneutrino versus the e^+e^- center of mass energy. The error bars reflect the statistical errors for an integrated luminosity of 200 fb^{-1} . (b) The values of $\Delta\chi^2$ versus $m_{\tilde{\nu}_\tau}$ for the energy scan from 425 GeV to 600 GeV, assuming an integrated luminosity of 100 fb^{-1} (circles) and 200 fb^{-1} (triangles). The curves are a fit through these points. Also shown are the 90% CL with which $m_{\tilde{\nu}_\tau}$ might be measurable. Here we have taken the test case to be the “data” and only shown the change in χ^2 .

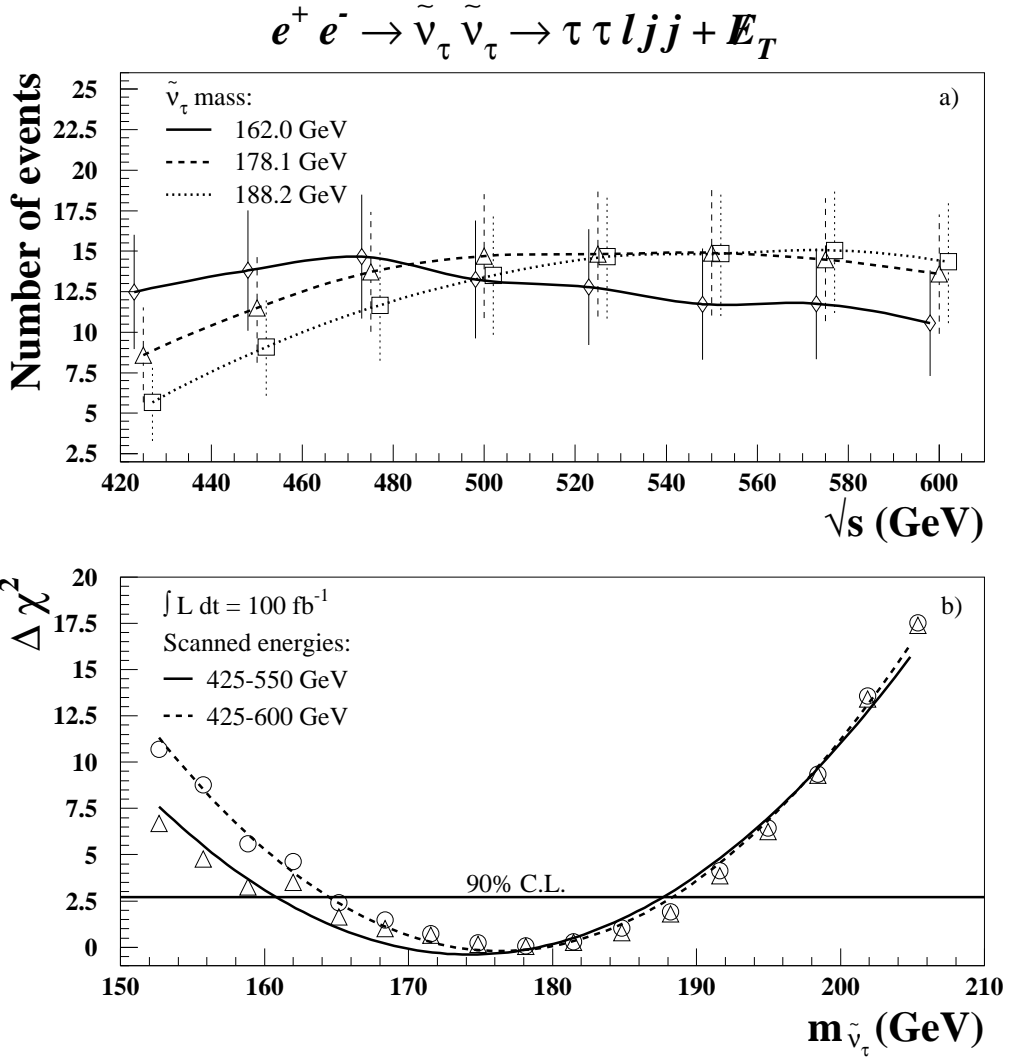


FIG. 9. The same as Fig. 8 except that the SUSY backgrounds are ignored and the integrated luminosity is fixed to be 100 fb^{-1} . Also in frame (b) we show the results for two sets of energy scans: from 425 GeV to 550 GeV in steps of 25 GeV (triangles) and from 425 GeV to 600 GeV (circles).